PS/RF Note 2000-019
CERN-NUFACT-NOTE 37

Design of the 120 MeV Drift Tube Linac for the SPL[1)]

Frank Gerigk, Maurizio Vretenar

Abstract

In the present design of the SPL a room temperature drift tube linac (DTL) accelerates the beam from 7 MeV up to an energy of 120 MeV. Two types of DTL are proposed for this energy range: a standard Alvarez structure covers the low energy part (7 - 18 MeV), followed by a cell-coupled 2-gap DTL structure (CCDTL) for the high energy part. Both sections operate at 352 MHz and make use of existing LEP klystrons. The layout is optimised for real estate shunt impedance and cost effectiveness. The results of RF field calculations and multiparticle simulations are presented, as well as the choice of parameters.

[1)] Superconducting Proton Linac

1 The Alvarez DTL

Two standard Alvarez tanks at 352 MHz accelerate the beam from 7 MeV up to 18.5 MeV. Focusing is achieved by a conventional FODO lattice with quadrupoles inside of the drift tubes. Both tanks are stabilised with post-couplers. The shape of the drift tubes in both tanks is mainly determined by the size of the quadrupoles. In order to avoid the high costs for a pulsed magnet power supply the quadrupoles work in continuous mode. This choice results in higher heat dissipation, enforces the use of hollow copper windings for the quadrupole coils, therefore enlarges the drift tubes (to 200 mm) and reduces the shunt impedance.
The aperture diameter of the tubes also affects the size of the quadrupoles and therefore the shunt impedance. An aperture radius of 10 mm has been chosen, resulting in a ratio between aperture and r.m.s. beam size between 8.5 and 10. These values are quite conservative, providing enough safety margin against the loss of possible halo particles, and at the same time keeping the tolerances for the alignment of the quadrupoles at realistic values.

Table 1: Geometrical parameters of the standard Alvarez tanks

	tank radius	**tank length**	**tube radius**	**tube length**	**aperture diameter**	**cells**	**magnet length**	**magnet aperture**	**stem radius**
tank 1	238 mm	4.29 m	100 mm	64 - 82 mm	20 mm	36	52 - 60 mm	24 mm	15 mm
tank 2	244 mm	3.95 m	100 mm	88 - 115 mm	20 mm	26	62 - 70 mm	24 mm	15 mm

The DTL cell geometries were optimized with the *SUPERFISH* [1] tuning code *DTLFISH* and are shown in Figure 1.

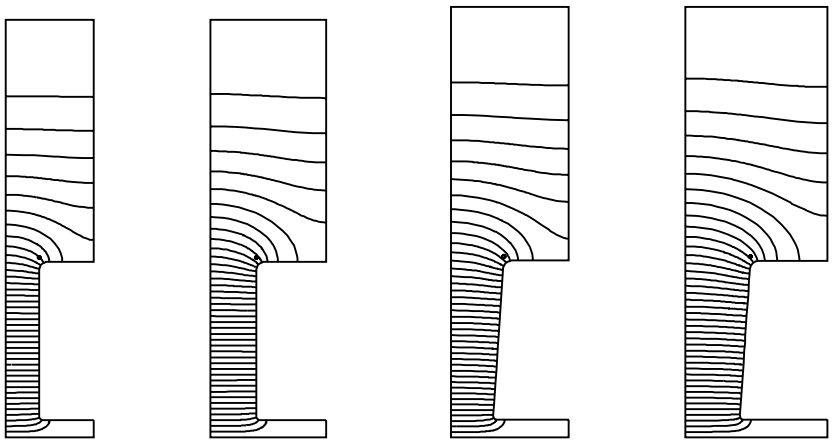

Figure 1: First and last DTL cells of each tank

Due to the choice of a DC magnet power supply and to the safety margin in the aperture the DTL shunt impedance is relatively low (see Figure 6). For this reason it is important to pass to the more effective cell-coupled structure as soon as possible. The transition criterion is the available magnet space between single CCDTL tanks. Since the coupled tanks operate in the $\pi/2$ mode the distance between tanks is an integer multiple of $\beta\lambda$.[1)] For a 60 mm long magnet a total length of 160 mm is required for mounting the quadrupole between the tanks. This yields a transition energy which is defined by: $\beta\lambda \approx 160$ mm ($\Rightarrow \approx 18$ MeV).
A synchronous phase of -38^o at the beginning of the DTL provides enough longitudinal acceptance for a proper capture of the beam. As shown in Figure 2 the longitudinal aperture ratio[2)] does not exceed a maximum value of 60 %. Towards the end of tank 1 the synchronous phase is reduced to -35^o and eventually reaches -30^o at the end of tank 2.

[1)] this corresponds to a distance of $1.5 \cdot \beta\lambda$ between adjacent gap centres of adjacent tanks

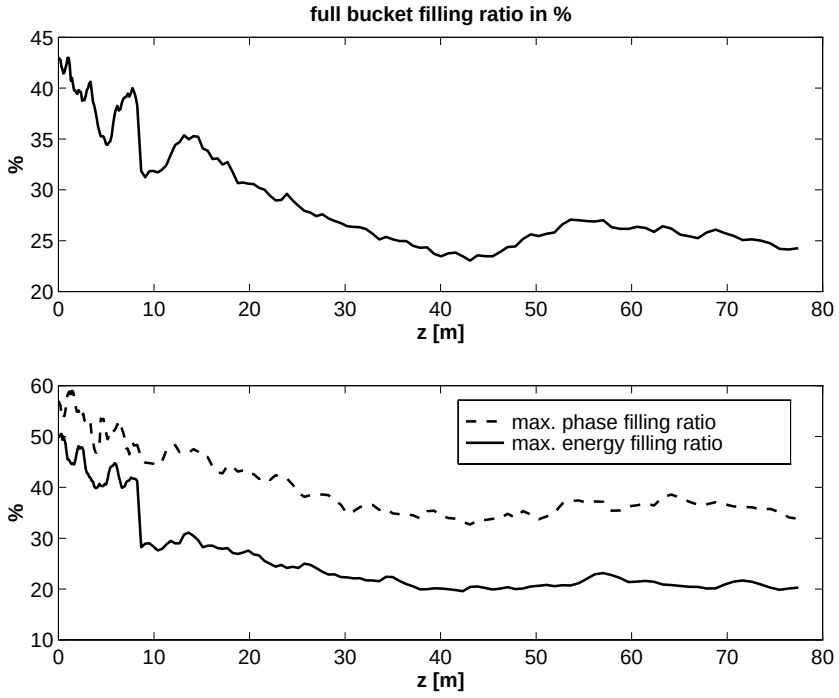

Figure 2: Filling ratios for full and half buckets

In the present design the overall gradient along the room temperature structure was chosen to be $\mathbf{E}_0 = 2.5$ MV. Since the transverse phase advance is quite low (see Fig. 3) a high gradient in the first DTL tank yields a high temperature ratio[3)] between particle oscillations in the longitudinal and the transverse plane. Multiparticle simulations with PARMILA [2] showed that temperature ratios above 4 often lead to transverse beam oscillations. Therefore the first tank starts with a gradient of 2 MV, which is then raised up to 2.5 MV towards the end. The transition energy between the tanks is chosen such that each tank can be fed by one LEP type klystron.

Table 2: RF parameters of the standard Alvarez tanks

	$\mathbf{W}_{in}$ [MeV]	$\mathbf{W}_{out}$ [MeV]	$\mathbf{E}_0$ [MV]	ϕ_s [deg]	$\mathbf{ZTT}^*_{av.}$ [MΩ]	Kilp. max.	$\mathbf{P}_{Cu}$ [kW]	$\mathbf{P}^{**}_{total}$ [kW]
tank 1	7	12.5	$2 \rightarrow 2.5$	$-38 \rightarrow -35$	14.9	0.58	734	794
tank 2	12.5	18.6	2.5	$-35 \rightarrow -30$	18.4	0.56	719	786

* including 20% reduction from SUPERFISH calculations
*the beam power is calculated for 11 mA (mean current during pulse)

A 3D field calculation of the first DTL cell has been performed with **GdfidL** [3] for two purposes, the first one being the comparison with the SUPERFISH results (Table 7) and the second one being a detailed loss calculation (Fig. 4). The 3D loss distribution can be transferred to a mechanical simulation code in order to check the deformation of the drift tubes under heat load. One can also see that the currents on the stem cause considerable losses, especially at the connection between stem and drift tube. At this energy the stem losses contribute about 10% to the overall losses per cell.

2) $\frac{\phi_{max.}-\phi_{sync.}}{\phi_{bucket-boundary}-\phi_{sync.}}$; $\phi_{max.}$ and $\phi_{bucket-boundary}$ are taken from the left half bucket

3) temperature ratio $= \left(\frac{\varepsilon_z}{\gamma \cdot z}\right)^2 \Big/ \left(\frac{\varepsilon_t}{r_t}\right)^2$

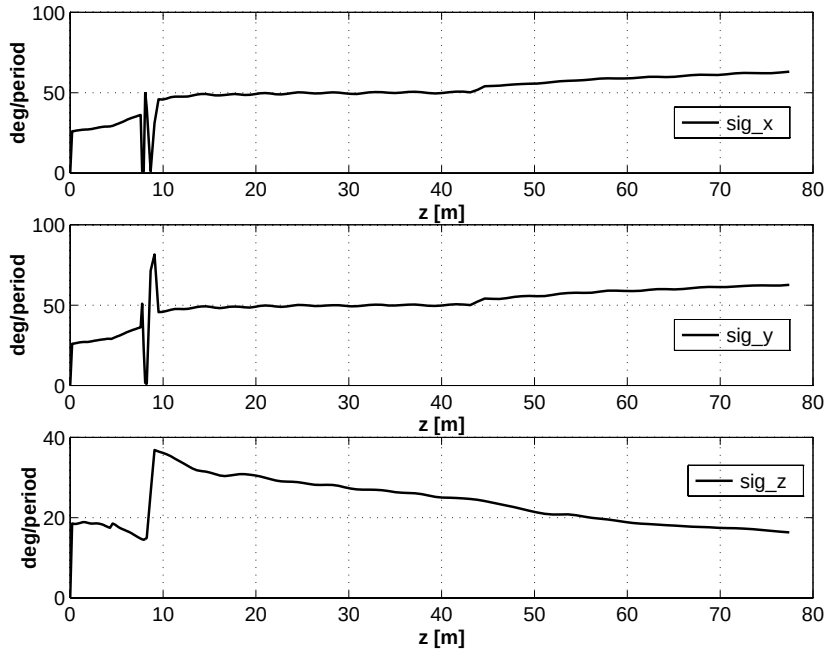

Figure 3: Longitudinal and transverse full current phase advance

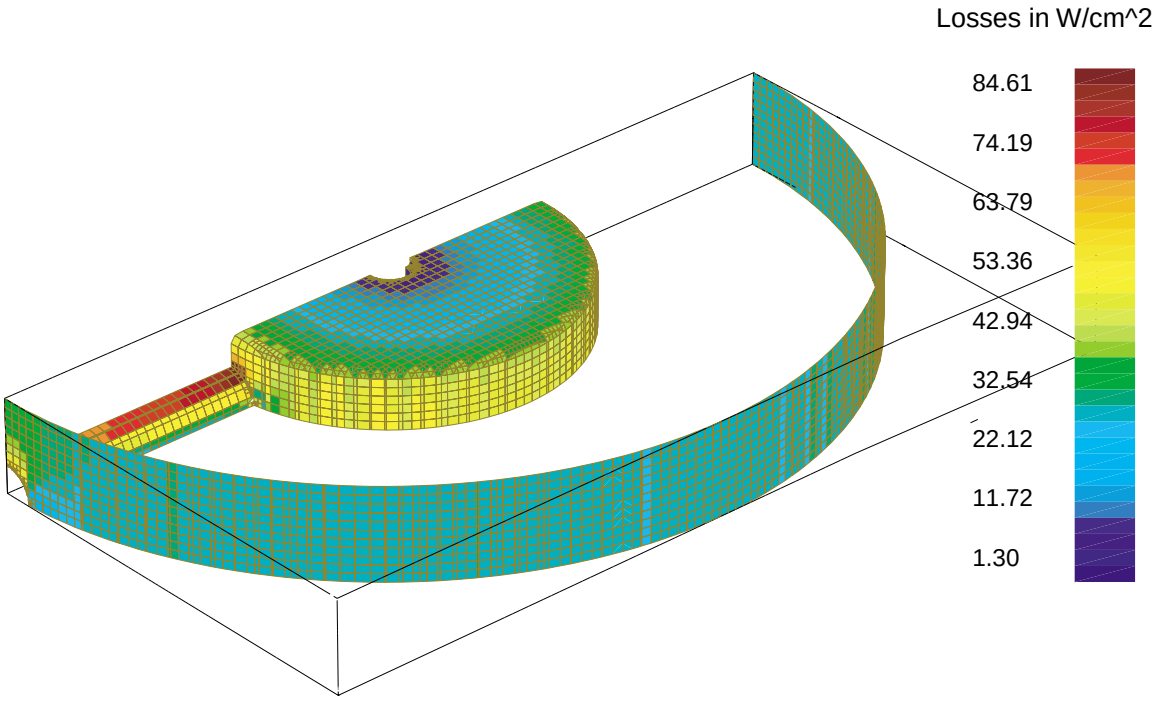

Figure 4: Distribution of losses in the first DTL cell

2 The cell-coupled DTL

From 18.5 MeV onwards the more effective cell-coupled DTL structure is used to further accelerate the beam, because due to the lower space charge forces a longer focusing period ($4 \cdot \beta\lambda$ in our case) becomes possible. The main advantages of DTL structures made of small tanks with external quadrupoles are the higher shunt impedance, due to the smaller diameter of the drift tubes, the lower construction costs, due to the simpler fabrication of the drift tubes and to the relaxed alignment tolerances, and the simpler alignment and cooling of the quadrupoles.

It is also expected that the relatively low duty cycle of the SPL (16.5%) will simplify most of the thermal problems, encountered when operating this type of structure in CW mode. The structure preferred for the SPL, the CCDTL (cell-coupled DTL), is based on the Los Alamos studies for the APT [4]. Short DTL tanklets with two gaps are connected by off-axis coupling cavities (Fig. 5). One 1 MW klystron can feed a chain of (max. 11) tanklets via a simple feeder placed in one of the tanklets. The input matching can be adjusted for different beam currents by a waveguide short circuit at $\lambda/4$ distance from the iris.
The focusing lattice is again FODO with quadrupoles between the tanklets. Since the magnets are no longer included in the vacuum tanks, the alignment and mounting becomes much easier. Also the construction and the cooling of the quadrupoles is facilitated because there are no spatial restrictions as in the drift tubes. Keeping FODO focusing all along the linac has the additional advantage that the beam can be matched at the transition between the Alvarez and the CCDTL without an additional matching line.

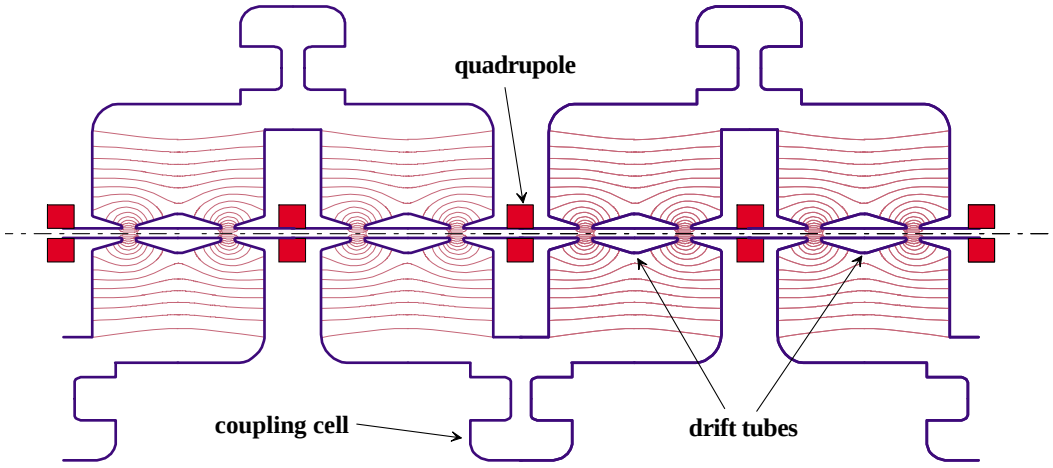

Figure 5: Scheme of the cell-coupled DTL structure

The coupled structure works in the $\pi/2$ mode, which means that there is ideally no field (and therefore no wall losses) in the coupling cavities. The shunt impedance calculated by SUPERFISH is reduced by a factor of 0.85 to account for imperfections and the effect of the coupling slots.
The "classical" two gap LANL structure has a constant tank length of $1.5 \cdot \beta\lambda$, while the proposed design for the SPL uses lengths between $1.5 \cdot \beta\lambda$ and $2 \cdot \beta\lambda$. Lengthening the tanks towards the high energy end of the CCDTL provides a constant space of 160mm (or 170mm; from 68 MeV onwards) for mounting the quadrupoles.
The advantages of this approach are:

- standardized mounting of the magnets,
- standardized design of coupling cavities for the whole CCDTL,
- no transitions in the transverse focusing lattice after the Alvarez DTL,
- higher real estate shunt impedance,
- high ratio of active structure length to total length, and
- short coupling cavities $\Rightarrow$ no problems with higher order modes in the coupling cavities.

In order to provide space for diagnostic elements, individual tanks can be shortened, for example at the end of each string of tanklets, without affecting the transverse focusing lattice. Figure 6 shows the beneficial effect of lengthening the tanks to $2 \cdot \beta\lambda$: while the shunt impedance of the CCDTL structure itself decreases rapidly, the real estate shunt impedance shows a broad maximum. Altogether the structure has an average effective shunt impedance of 33MΩ/m. Table 4 gives a summary of the RF properties.

Table 3: Geometrical parameters of the CCDTL

tank radius [mm]	**tank length [mm]**	**tube radius [mm]**	**aperture radius [mm]**	**tube length [mm]**	**stem radius [mm]**	**tanks**	**magnet length [mm]**	**total length [m]**
238 → 290	253 → 787	42.5	12	147 → 275	10	98	60/70	69.6

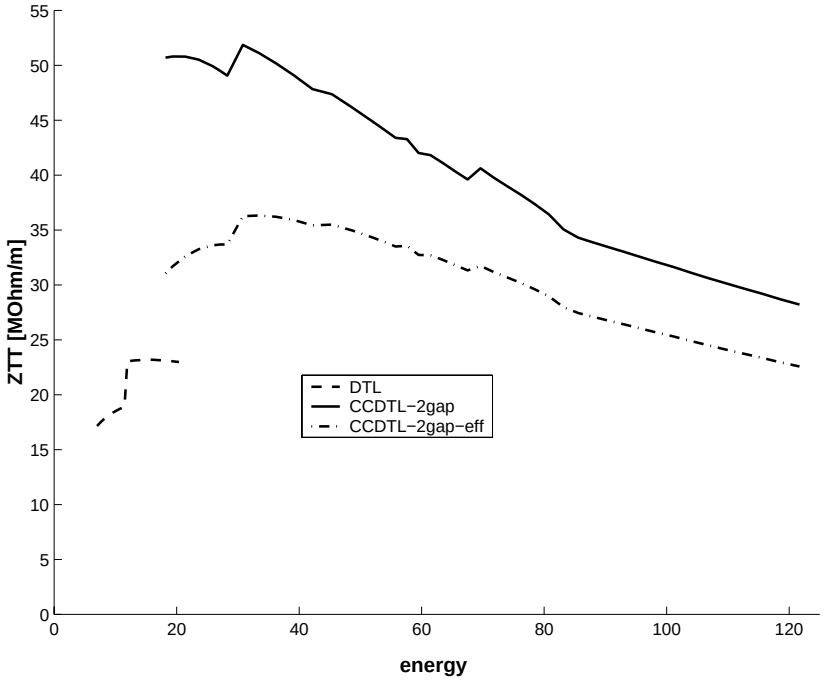

Figure 6: Shunt impedance calculated by SUPERFISH (without reduction)

Table 4: RF parameters of the CCDTL

$\mathbf{W}_{in}$ [MeV]	$\mathbf{W}_{out}$ [MeV]	$\mathbf{E}_0$ [MV]	ϕ_s [deg]	$\mathbf{ZTT}^{*}_{av}$ [MΩ]	**Kilp. max.**	$\mathbf{P}_{Cu}$ [MW]	$\mathbf{P}^{**}_{total}$ [MW]	$\mathbf{n}_{klystrons}$
18.6	120.1	2.5	-35 → -25	33	1.75	5.943	7.06	9

* including 15% reduction from SUPERFISH calculations
*the beam power is calculated for 11 mA (mean current during pulse)

2.1 Design of the coupling cavities

The coupling cavities were designed using the 3D eigenvalue solver of Gdfidl [3]. Two different types have been designed and tested: one for 160 mm spacing between the CCDTL tanks and one for 170 mm. Both cavities were tuned to the same frequency as the CCDTL and then coupled to the tanks by coupling slots. The size of the coupling slots determines the coupling factor and the loss in shunt impedance caused by the coupling.
In order to determine the dependency of the shunt impedance reduction from the coupling factor, the overlapping volume between CCDTL tanks and coupling cavities has been varied by moving the coupling cells gradually towards the beam axis (see Fig. 8). Figure 7 indicates a ratio of ≈4% reduction in shunt impedance per each percent of coupling. Due to the low number of cells in the chain, the power flow droop remains low even for small values of the coupling factor. A 2% coupling (8% reduction in shunt impedance) gives a power flow droop of only about 0.1%.

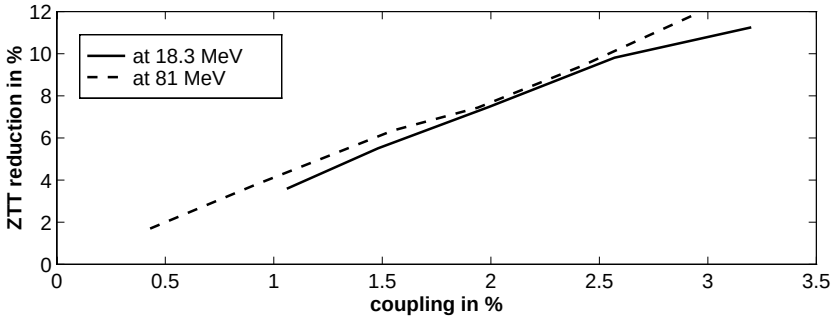

Figure 7: Reduction of shunt impedance for coupled CCDTL tanks

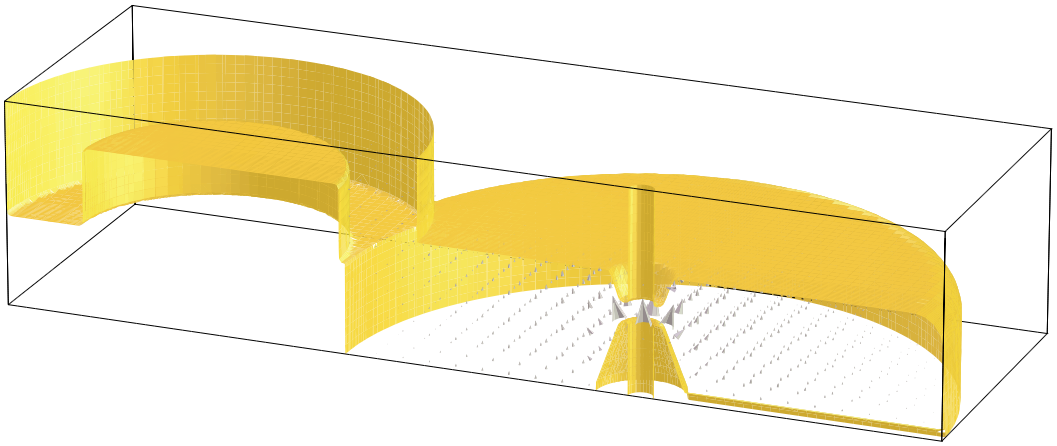

Figure 8: Gdfidl model for the CCDTL

3 Beam Dynamics

The beam dynamics simulations have been performed with PARMILA [2], using 25000 particles in a 6D waterbag distribution. TRACE3D [5] has been used for matching. The beam current for the simulations was set to 40 mA, to leave a margin from the SPL bunch current of 18 mA. The transition between the Alvarez DTL and the CCDTL is matched by varying the quadrupoles and the synchronous phases in the transition area. Due to the restrictions for the size of the quadrupoles (see section 1) the transverse phase advance at the beginning of the DTL is relatively low. Starting with $\sigma = 26^0$ ($\sigma_0 = 33.5^0$) the phase advance is raised up to $\sigma = 63^0$ ($\sigma_0 = 69.5^0$) towards the end of the CCDTL (see Fig. 3).

One of the design guidelines was to keep the temperature ratio below 4, to avoid the excitation of parametric beam resonances. At 7 MeV this factor is close to 4 and is then reduced towards 1 at the output of the linac. The r.m.s. emittances as well as the 90% emittances are remarkably stable. (Table 5). As shown in Figure 9 the maximum beam size is below 4.5 mm in the CCDTL (and below 3.2 mm in the Alvarez DTL), yielding a ratio of 2.7 (3.1) between the total beam size and the aperture. Even an input beam with 30% mismatch (beam radius) in all three planes is well kept inside the aperture. The maximum transverse beam size for the mismatched beam did not exceed a value of 8 mm (maximum r.m.s. radius: 2.1 mm).

4 High gradient version

A second version of the linac has been designed for a gradient of E_0 =3 MV/m. The mechanical and the RF properties of this version are basically the same as for the 2.5 MV/m version, apart from the shorter length and the higher power consumption. The CCDTL tanks had to be slightly redesigned in order to keep the maximum Kilpatrick value below 1.8. For the beam dynamics simulation, the matching section between the Alvarez DTL and the CCDTL has also been

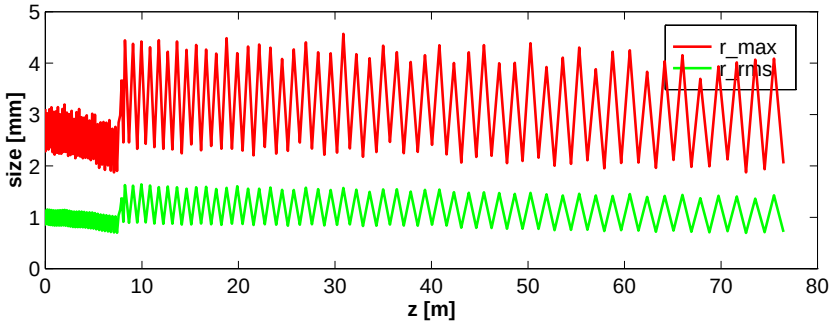

Figure 9: Transverse beam size along the linac (matched case)

Table 5: Beam data for the nominal- and the mismatched beam (30% mismatch)

	in	**out**	**mism. out**	**unit**
$\varepsilon_{x,y;rms;norm}$	0.26	0.26	0.35	[π mm mrad]
$\varepsilon_{x,y;90\%;norm}$	1.11	1.13	1.45	[π mm mrad]
$\varepsilon_{z;rms}$	0.59	0.59	0.60	[π deg MeV]
$\varepsilon_{z;90\%}$	2.54	2.53	2.44	[π deg MeV]
rms beam radius x,y	1.15	1.43	2.10	[mm]
rms phase spread	$\pm$ 9.4	$\pm$ 3.6	$\pm$ 3.1	[deg] at 352.2 MHz
rms energy spread	$\pm$ 63	$\pm$ 167	$\pm$ 207	[keV]

redesigned. The resulting beam properties are essentially the same as for the 2.5 MV version. Table 6 lists the differences between both versions.

Table 6: Differences between the 2.5 MV/m linac and the 3 MV/m linac

gradient	**total length**	**power consumption**	**number of klystrons**
2.5 MV/m	78 m	8.64 MW	11
3.0 MV/m	66 m	10.4 MW	13

Table 7: Comparison between SUPERFISH and GdfidL results for the first DTL cell

	ZTT [$M\Omega/m$]	**ZTT/Q** [Ω]	**Q**	**f** **[MHz]**	**P**$_{Cu}$ **[kW]**
SUPERFISH	17.15	23.5	37 710	352.2 (354.25*)	11.53
GdfidL	16.75	23.8	36 390	355.5	12.06

* SUPERISH estimation for the frequency, when taking into account the effect of the stem

References

[1] James H. Billen and Lloyd M. Young. *Poisson Superfish, LA-UR-96-1834.* LANL, Revised 1999.

[2] Harunori Takeda. *PARMILA, LA-UR-98-4478.* LANL, 1999.

[3] Warner Bruns. *Improved GdfidL with Generalized Diagonal Fillings and Reduced Memory and CPU Requirements.* ICAP 98, 1998.

[4] J. Billen; F. Krawczyk; R. Wood; L. Young. A New RF Structure for Intermediate-Velocity Particles. In *Linac 94*, page 341, 1994.

[5] D.P. Rusthoi K.R. Crandall. *TRACE 3-D Documentation, LA-UR-97-886.* LANL, 1997.